PCCP

Absorption Spectra of Pyruvic Acid in Water: Insights from Calculations for Small Hydrates and Comparison to Experiment

Journal:	*Physical Chemistry Chemical Physics*
Manuscript ID	CP-ART-04-2020-001810.R1
Article Type:	Paper
Date Submitted by the Author:	15-May-2020
Complete List of Authors:	Shemesh, Dorit; Hebrew University of Jerusalem, Chemistry Luo, Man; University of California San Diego Grassian, Vicki; University of California San Diego, Gerber, Robert; The Hebrew University of Jerusalem , Chemistry; University of California, Irvine,

Absorption Spectra of Pyruvic Acid in Water: Insights from Calculations for Small Hydrates and Comparison to Experiment

Dorit Shemesh[1], Man Luo[2], Vicki H. Grassian[2], R. Benny Gerber[1,3]

[1]Institute of Chemistry, Fritz Haber Research Center, Hebrew University of Jerusalem, Jerusalem 91904, Israel

[2]Department of Chemistry, University of California, San Diego, CA 92093, USA

[3]Department of Chemistry, University of California, Irvine, CA 92697, USA

Abstract

Pyruvic acid is abundant in the atmosphere and in seawater, being a decay product of living organisms. Although very small in size (10 atoms), pyruvic acid exhibits conformational complexity in the gas phase and in solution, which is reflected in the UV spectrum. The gas phase UV spectrum of pyruvic acid differs from the spectrum of pyruvic acid in water. The main atmospherically relevant absorption peak in the gas phase is blue shifted by about 0.43 eV (40 nm difference in the peak location) in water. The origin of the blue shift has not been established thus far. This paper aims at a microscopic understanding of the absorption spectrum of pyruvic acid in aqueous media by a combined experimental and theoretical approach. ^{1}H NMR experiments were performed to reveal the contribution of the different conformers in solution as a function of pH. Computationally, hydrates of sizes up to 5 water molecules using two different species of pyruvic acid, the neutral acid and the anionic form were considered. Vertical excitation energies using the ADC(2) method (algebraic-diagrammatic construction through second order) of these structures provide insights into the blue shift of the atmospherically relevant absorption peak. Additionally,

molecular dynamics simulation on MP2 (Møller-Plesset perturbation theory**)** ground state of small clusters of pyruvic acid with four water molecules were calculated and used in computing the vertical excitation spectrum along the dynamics. This is found to describe very accurately the experimental spectrum. Overall, the results show that small hydrate models including the roles of both neutral and deprotonated speciated forms provide a good quantitative description and a microscopic interpretation of the experimental spectrum of pyruvic acid in aqueous solution.

Introduction

Atmospheric chemistry has evolved as a major field of science since it provides a molecular understanding of significantly and globally debated environmental changes in air quality and climate[1–3]. Aerosols are important constituents of the atmosphere and are therefore of essential research interest. From a molecular point of view, aerosols are very complex and involve different components with many containing a variety of organic molecules. It is therefore crucial to have a deeper understanding of each individual component, in order to facilitate the understanding of these complex systems. One important component in aerosols is pyruvic acid. Pyruvic acid has a high abundancy in the atmosphere[4–6] since it is a key intermediate in metabolic pathways in living organisms and is therefore emitted to sea water and to the atmosphere. Other sources of pyruvic acid include biomass burning[7,8], photooxidation of aromatics[9,10] and oxidation of isoprene[11–13]. Photochemical reactions of pyruvic acid has been extensively studied experimentally such as gas-phase and condensed-phase photolysis[14,15,24–29,16–23] .Theoretical studies investigated structural conformers of pyruvic acid and pyruvic acid-water complexes and their reactions, excited state dynamics and deactivation pathways and barriers to decarboxylation[30–39]. Since mineral dust aerosols are abundant in the atmosphere, the interaction of pyruvic acid with silica surface has been studied as well[40].

Identification of different species can be performed by recording their photoabsorption spectra. The photoabsorption spectra are sensitive to the structures of molecules and to their environment and are therefore able to distinguish and to identify different conformers. Additionally, solvents such as water lead to speciation of molecules, as for example neutral acid and its deprotonated anionic form. The pH of the solution effects the composition of these different protonation states in solution. The photoabsorption spectrum is therefore a key tool for characterizing the different

structural conformers and species that might co-exist in gas phase and solutions. Quantum chemical calculations support the analysis of the experimental spectrum by providing a molecular picture of the species involved. Knowledge of the structure and composition is the first step for understanding photoinduced reactions of atmospheric species[41–43].

Macroscopic properties such as pH present a challenge for computational models, since small clusters might not represent correctly the right ratio of protons and solute molecules (acid and base) in solution. The photoabsorption spectrum of pyruvic acid is impacted by different conformers and different species as outlined below and presents therefore a demanding task for computational models.

Although pyruvic acid is considered a relatively small molecule with 10 atoms, it has several structural conformers, due the possibility of intramolecular rotation around the C-C and C-O bonds[32,44,45]. IR spectroscopy of the different conformers has been recorded by Reva et. al[46]. Computationally, the different conformers and their energies were also elucidated[32,33,46–50]. Four different gas phase structures were identified. Figure 1 shows the two lowest energy structures, labeled Tc and Tt, Tc being the global minimum. The lowest conformer has an additional stabilization due to the intramolecular hydrogen bond between the acidic hydrogen and the α-carbonyl.

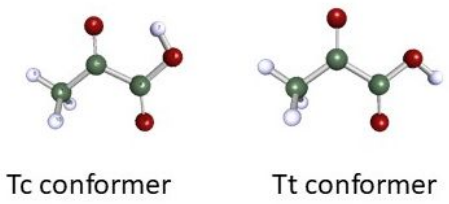

Figure 1: Lowest energy structures of pyruvic acid in the gas-phase, Tc conformer and Tt conformer. The Tc conformer is the global minimum of pyruvic acid in the gas phase.

The other conformers differ in the C-C-C=O angle (upper-case letter C, Cis; T, Trans) and the C-C-O-H angle (lower-case letter c, cis; t, trans). The Ct and the Tt conformers are higher in energy than the Tc conformer by at least 2 kJ/mol (up to 12 kJ/mol, depending on the level of calculation). The Cc conformer is much higher in energy, and therefore not populated at room temperature.

Experimentally, the lowest energy conformers Tc and the Tt conformer were detected by different techniques[44,46,51,52]. Additionally, to all the mentioned conformers, which are all rotational isomers of the Tc conformer, pyruvic acid exhibits keto-enol tautomerism. However, only a few studies have characterized the enol tautomers experimentally and theoretically[34,36,48]. The keto-enol tautomerism pathways were studied theoretically for the gas-phase pyruvic acid, and for the pyruvic acid – water complex[36]. Water is shown to diminish the barrier for keto-enol tautomerism[34]. In apolar solvents FTIR spectra of pyruvic acid combined with computational analysis of the relevant structures, show the existence of one enol form, besides three keto forms[48]. The enol form, as stated above, has only been characterized by a few experiments. Raczynska et al.[48] has calculated the energy barrier for keto-enol tautomerism to be about 40 kJ/mol, experimental values reduces this value to 36 kJ/mol for completely hydrated structures[53]. Therefore, we have not addressed the enol form in our study.

In aqueous solution, pyruvic acid exists in four different structural forms[54]: neutral and anionic pyruvic acid and their hydrated forms (diols) respectively, see Figure 2. The protonated form of pyruvic acid is its ketone neutral form. Upon hydration of the ketone, the resulting species becomes a geminal diol. Both the ketone and diol species can be deprotonated to an anionic form.

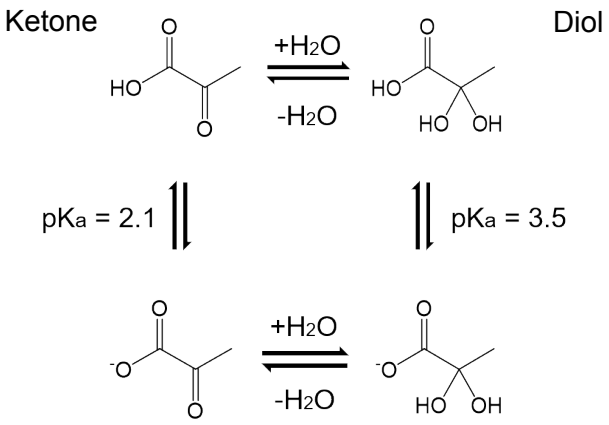

Figure 2: Four forms of pyruvic acid in aqueous solution. pKa values has been obtained from our previous study[55].

Most interesting is that the photochemical properties of these four forms are found to be very different.[23]The percentage distribution of the four forms depends on the pH of the solution. Besides

higher pH favoring the anionic forms and lower pH the acidic forms, higher pH favors the ketone and lower pH the diol.

Both gas phase and aqueous phase exhibit therefore a great deal of conformational diversity. Experimentally, the structural differences can be elucidated using spectroscopic signatures of the various pyruvic acid, e.g. through IR or UV. Synergistically, computations add in the interpretation of the spectra and the identification of the conformers. Ideally, molecular simulation of solvated pyruvic acid in a large cluster of water molecules will show the transition between the different species, and calculation of the spectra from this simulation should be able to reveal all the spectroscopic characteristics of pyruvic acid. However, this approach is computationally unfeasible. Therefore, we hope that a molecular approach based on small clusters with up to five water molecules can recover the main features of the spectrum. This is based on the assumption that a small number of different speciated forms embedded in water clusters with up to five water molecules will correctly represent the local environment of the speciated forms in solution.

There are several approaches for treating how solvation affects molecular electronic transitions and the UV spectrum[56]. One useful method is to use a polarizable continuum model (PCM) for studying the electronic properties of solvated molecules[57]. However, this macroscopic continuum model lacks the microscopic information on the arrangement of solvent molecules around the molecule, and their intermolecular interaction such as hydrogen bonds. Another method often used is quantum mechanics/molecular mechanics (QM/MM) simulation[58,59], in which solvent molecules are explicitly treated, although the computational costs associated with this method is much more expensive than our approach outlined below. Lastly, good agreement has been also found by applying the RISM-SCF-SEDD Theory for providing vertical excitation energies for gas phase and water solvated p-coumaric acid[60].

The main peak in the UV spectrum of pyruvic acid in the atmospherically relevant region (higher than 290 nm) is blue shifted from 360 nm in the gas phase to 320 nm in the aqueous phase[21,23,61–63]. In both cases, the excitation is mainly an n to π^* excitation but this large shift is poorly understood. Therefore, the objective of this paper is to provide insight into the effect of water on the spectrum of pyruvic acid by a combined experimental and theoretical approach. The theoretical approach will investigate the spectrum in terms of a small number of speciated forms of pyruvic acid in small clusters, each aim to represent a local configuration of the system in solution at a

given point in time. Experimental data will provide insight into the relative role of anionic and neutral speciated forms at different pH. The comparison of the theoretical prediction with the measured spectra should be an indication of the success of this approach to provide microscopic understanding of the spectra in terms of molecular structures. A similar approach has been successfully employed recently for the study of the absorption spectra of benzoic acid in water[64]. Other related approaches include for example the calculation of the UV spectrum of malonaldehyde in water (solvation is modeled by using a solvation model based on density)[65] and the calculation of the UV spectra of tautomers of different nucleobases by a semi-classical ab initio spectra simulation[66].

Methodology

1. Theory

Gas-phase structures:

As discussed in the introduction, only the Tc and Tt conformers are available in the gas phase in significant amount. Therefore, we have only considered both structures for calculating excitation energies for simulating the gas phase UV spectrum. The structures are depicted in Figure 1.

Hydrates of speciated forms of pyruvic acid:

The lowest energy conformer, Tc (see Figure 1), was used for the ketone structure of pyruvic acid. Additional clusters with water molecules were built by starting with the Tc conformer and adding each time one water molecule. Clusters with up to five water molecules were built in this way. The structures were then optimized. The same was done for the anionic form of pyruvic acid. The diol forms were not considered in the calculations, since both forms are not observed in the atmospherically relevant region (above 290 nm) (see Tables 3 and 4 in the Results section). Vertical excitation energies of several monohydrated structures of the ketone and the anion diol confirms that hydration does not dramatically alter the peak location, see Supporting Information for more details. Our objective was to show, that a minimalistic cluster approach is enough to correctly reproduce the UV spectrum. Insights can be gained for the structure of the solvated

pyruvic acid, on the ratio between different speciated forms, and on the location of the electronic excitation involved. Figure 3 shows the structures of the anionic clusters under consideration.

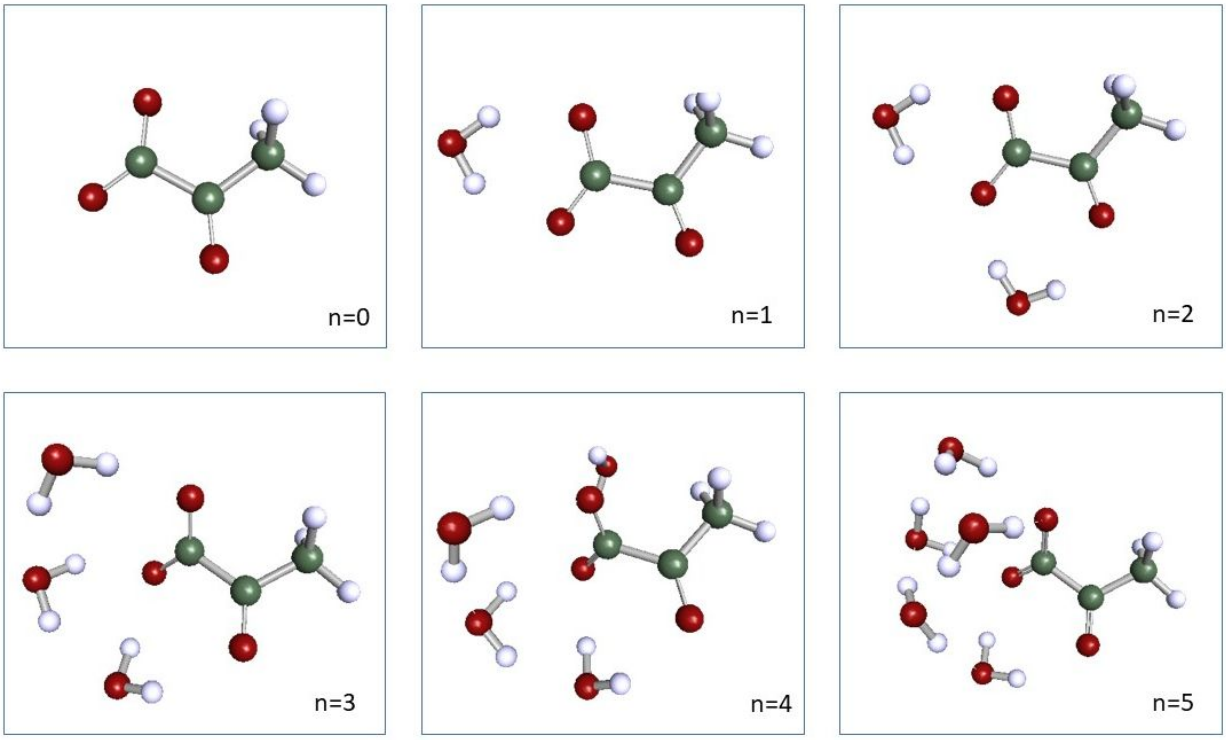

Figure 3: MP2/cc-pVDZ optimized anion clusters with n=0,1,2,3,4 or 5 water molecules

The anionic clusters were built by adding one water molecule at a time and optimizing the structure. The first structure has one water molecule which is located at the COO- group and which makes hydrogen bonds between both oxygens of the anion and both hydrogens of the water molecule. This is the preferred location for the water molecule, since it stabilizes the negative charge. Additional water molecules are then added and are located near the additional oxygen. The water molecules are located around the oxygens since those bonds are more polar than the C-H bond of the methyl group. The methyl group is hydrophobic and is therefore not involved in hydrogen bonds. At larger cluster sizes this is clearly seen, by accumulation of the water molecule on one side of the anion only. Figure 4 shows selected structures for the neutral/protonated ketone form.

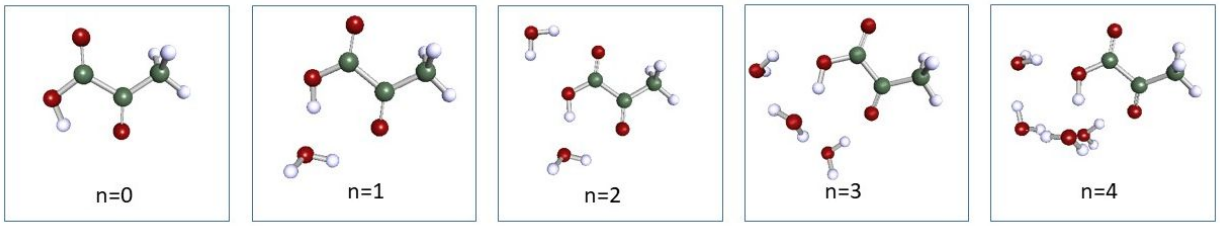

Figure 4: MP2/cc-pVDZ optimized structures of neutral ketone and ketone with water clusters. n is the number of water molecules, clusters with n=0, 1, 2, 3 or 4 water molecules are shown

The clusters were built by adding one water molecule and optimizing the structure. The structure for pyruvic acid and one water molecule is similar to the structure published by Schnitzler et al.[37]. The structure of pyruvic acid with two water molecules is similar to the one published by Kakkar et al.[34]. For consistency, we have considered structures built by adding water molecules to the Tc conformer only. The Supporting Information shows the structure and the optical properties for the Tt conformer with two water molecules. The optical properties are very similar, the excitation energy differs only by a few nm. The water molecules which are added are hydrogen bonded to the oxygens and to the hydrogen of the hydroxyl group. The methyl group does not attract water molecules, as discussed above.

Potential energy surfaces: Ground state calculations: Structures were optimized using the MP2 potential with a cc-pVDZ basis set. A smaller basis set (def-SV(P)) was used for running molecular dynamics on pyruvic acid with water, since the energies needs to be evaluated many times, and the cc-pVDZ basis set would be too costly for this.

Potential energy surfaces: Excited state calculations: Two kinds of methods were employed for calculating the UV spectrum of gas phase and solvated pyruvic acid. In the first method only the vertical excitation energies and their optical properties in the Franck-Condon region were evaluated. Excitation energies were calculated using the ADC(2) method. The ADC(2) method has been used in previous studies by our group and has been proven to be accurate for spectrum calculations and for photochemical reaction dynamics of atmospherically relevant organic systems.[41–43,67,68] The difference for different basis set employed (def-SV(P) and cc-pVDZ) in energy and optical properties was not significant (see Supporting Information for gas phase pyruvic acid). For excited states calculated at the ADC(2) level, the transition density between the

ground state and an excited state can be transformed to a diagonal form through a singular value decomposition of the excitation amplitudes[69,70]. From the transformation, natural transition orbitals are obtained which are used in order to visualize the transition. Molecular orbitals are kept in the tables for labeling the transitions, and those can be found for selected transitions in the Supporting Information.

The second method was employed when static calculations (i.e. vertical excitation energies for optimized structures) were not sufficient for the description of the UV spectrum. This was the case for the solvated pyruvic acid. A dynamical approach was therefore necessary in order to sample more and different configurations. Molecular dynamics simulation using the MP2 potential ground state potential were done on both the anionic and the ketone cluster with 4 water molecules for 20000 au of time (=9.6 ps). Vertical excitation energies were calculated using ADC(2) method with the def-SV(P) basis set for 100 structures from the MD simulation . The smaller basis set was used since running molecular dynamics simulations on these systems are very costly and are only feasible with a smaller basis set. The resulting spectrum was smoothened by using a Lorentzian with a full width at half maximum (FWHM) of 0.15 nm. All the methods used are implemented in the Turbomole program suite.

2. Materials and Experimental Methods

Pyruvic acid (98%) was purchased from Sigma-Aldrich and distilled under reduced pressure. Aqueous solutions were prepared using Milli-Q water with an electric resistance of 18.2 MΩ. Pyruvic acid was prepared as 10 mM solutions. Solution pH was determined from an Oakton 700 pH meter and was adjusted by either hydrochloric acid (1 N stock solution, Fisher Chemical) or sodium hydroxide (1 N stock solution, Fisher Chemical).

UV-vis spectroscopy of the samples was taken using a PerkinElmer Lambda 35 UV-vis spectrometer with a wavelength range of 200 to 700 nm. ^{1}H NMR experiments for determining the ratio of ketone and diol forms of pyruvic acid at different pH were performed using a 300 Bruker AVA NMR spectrometer with wet suppression of H_2O. The ketone form methyl hydrogens have a ^{1}H NMR peak at ~2.4 ppm while for the diol form the methyl hydrogens are at ~ 1.6 ppm.[71] The ratio of protonated and deprotonated species was obtained from the pK_a of ketone and diol forms. The

calculation for the pK_a of ketone and diol forms of pyruvic acid in water solution has been discussed previously[55], see also reference.[71]

Results and Discussion

1. Pyruvic acid in the gas phase

The UV-vis spectrum of pyruvic acid in the gas phase was measured by several groups[21,61,62]. The main peak in the atmospherically relevant region lies at around 360 nm. Four different rotamers of pyruvic acid exists, whereas the Tc rotamer in Figure 1 has the lowest energy. We have adapted the nomenclature introduced by Räsänen et al.[32]. The uppercase letter (T, trans = 180° and C, cis = 0°) refers to the O=C-C=O dihedral angle and the lowercase letter (t, trans = 180° and c, cis = 0°) refers to the C-C-O-H dihedral angle. Experimentally, most of the studies have detected only the Tc rotamer[46,72–75], whereas some were able to identify the Tt rotamer as well[32,46]. Theoretically, the energy difference calculated by MP2/cc-pVDZ between the Tt and the Tc conformer is 0.09 eV, which leads to a Boltzmann distribution of only 3% for the higher lying Tt conformer. Similarly, in the experimental work of Reva et al. the abundance of the Tt conformer in a matrix at an even higher temperature (480 K) was still below 10%. Additional rotamers were predicted to lie at least 0.1 eV higher than the Tt conformer and were therefore not considered in this study. The experimentally peak at 360 nm can be explained by both the Tc and the Tt conformers, see Tables 1 and 2. Both structures absorb around 360 nm (i.e. 358 nm for the Tc conformer and 363 nm for the Tt conformer). Our calculations are therefore in excellent agreement with the experiment. Our results are also in good agreement with previously calculated excitation energies at different DFT (density functional theory) levels, most of them predicting a transition around 350 nm[30]. The second state (at around 235 nm) for both conformers is tabulated as well, in order to demonstrate, that there is no other relevant nearby excited state, which might contribute to the peak at 360 nm. The second excited state has a much larger oscillator strength by two to three order of magnitudes depending on the conformer, which explain the rise of the large peak starting at 300 nm towards lower wavelengths in the experimental spectra[21,61,62].

Table 1: ADC(2)/cc-pVDZ vertical excitation energies and optical properties for the global minimum conformer Tc of pyruvic acid.

State	Energy (eV)	Energy (nm)	Orbital Excitation	Description	Oscillator strength	Dipole moment (Debye)
S1	3.47	358	HOMO → LUMO 93 %	nπ*	0.00000035	1.862
S2	5.28	235	HOMO-2 → LUMO 84 %	nπ*	0.00044061	1.333

Table 2: ADC(2)/cc-pVDZ vertical excitation energies and optical properties for the Tt conformer of pyruvic acid.

State	Energy (eV)	Energy (nm)	Orbital Excitation	Description	Oscillator strength	Dipole moment (Debye)
S1	3.42	363	HOMO → LUMO 92 %	nπ*	0.00000077	0.397
S2	5.27	235	HOMO-3 → LUMO 84 %	nπ*	0.00023753	4.078

Figure 5 shows the natural transition orbitals that are involved in the excitation to the first excited state in the Tc and the Tt conformer. Molecular orbitals involved in the first excited state (corresponding to the label in Table 1 and 2) can be found in the Supporting Information. The orbital excitation is best described as a nπ* transition. The orbitals are very similar and are located on the common structural part of both conformers. The experimental peak can therefore be explained by both structures, however the much larger Boltzmann distribution of the Tc conformer compared to the Tt conformer, makes the main contribution of the Tc conformer to the experimentally observed peak more likely.

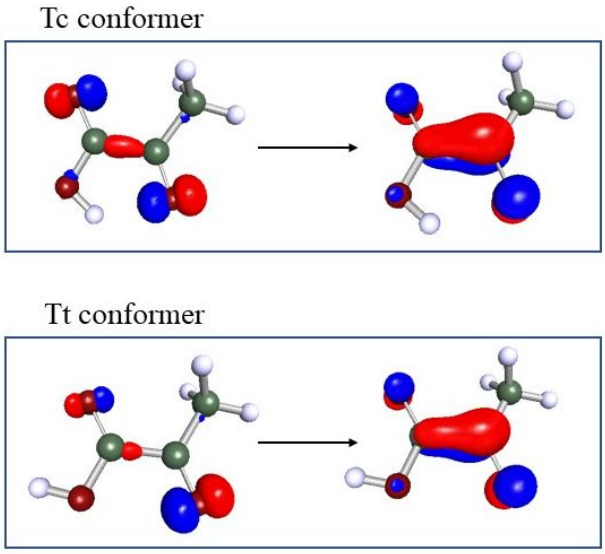

Figure 5: Occupied and virtual natural transition orbitals for the Tc and the Tt conformer of pyruvic acid.

2. Pyruvic acid in aqueous solution

The experimental UV spectra of pyruvic acid as a function of pH is shown in Figure 6. The UV spectrum of pyruvic acid in aqueous environment shows similar spectral lineshape as pyruvic acid in the gas phase, but the main peak is shifted by about 0.43 eV (40 nm difference in the peak location) towards the blue. In the atmospheric relevant region (above 290 nm) there is one main peak with maximal absorbance around 320 nm. A second peak starts to rise below 300 nm and has higher absorbance than the first peak. Our experimentally recorded UV spectrum for pyruvic acid in water is consistent with other UV spectra published in the literature[23,63]. Our objective of this study is to understand the spectral shift of about 40 nm that is induced by the aqueous environment. Figure 6 also shows the effect of the pH on the UV spectrum. The peak location is only shifted by a few nm due to the change in pH. Higher pHs shift the maximum of the peak towards the lower wavelength region. The absorbance at all wavelength are found to be higher when the pH increases. Although there is an observed effect of the pH on the spectrum, as discussed above, our objective of this current study is to model the effect of solvation on the peak location. Our theoretical models of small hydrates are not accurate enough for modelling the absorption spectrum at different pHs.

For the different pHs, the solution will consist of different ratios of PA, PA-, water and hydronium ions. In order to correctly model this scenario, very large clusters need to be employed, that consists of the correct ratio of all involved species at a given pH value. This consists of a series of very demanding calculations which is outside the scope of this study.

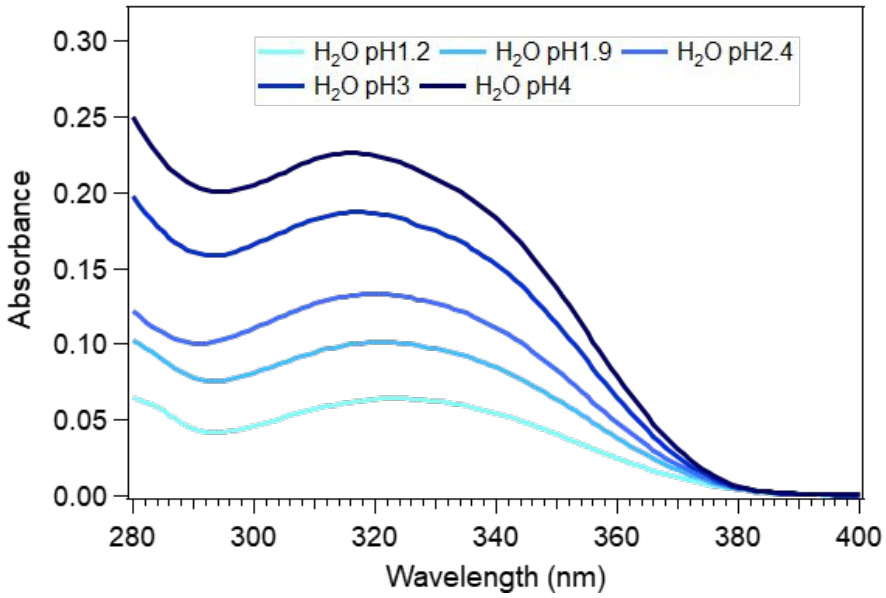

Figure 6: UV spectra of 10 mM pyruvic acid in water at different pH.

As discussed, pyruvic acid is known to exist in four different forms in the aqueous phase (see Figure 2). These four species and their monohydrates have been identified using vibrational spectroscopy in a water-restricted environment[54]. The ratio between the four different species as a function of pH has been recorded by Rapf et.al[23]. We have determined the ratio between the four different species using ^{1}H NMR spectroscopy. The relative contributions of all four species – ketone anion, ketone neutral, diol anion and diol neutral –is shown as a function of solution pH in Figure 7.

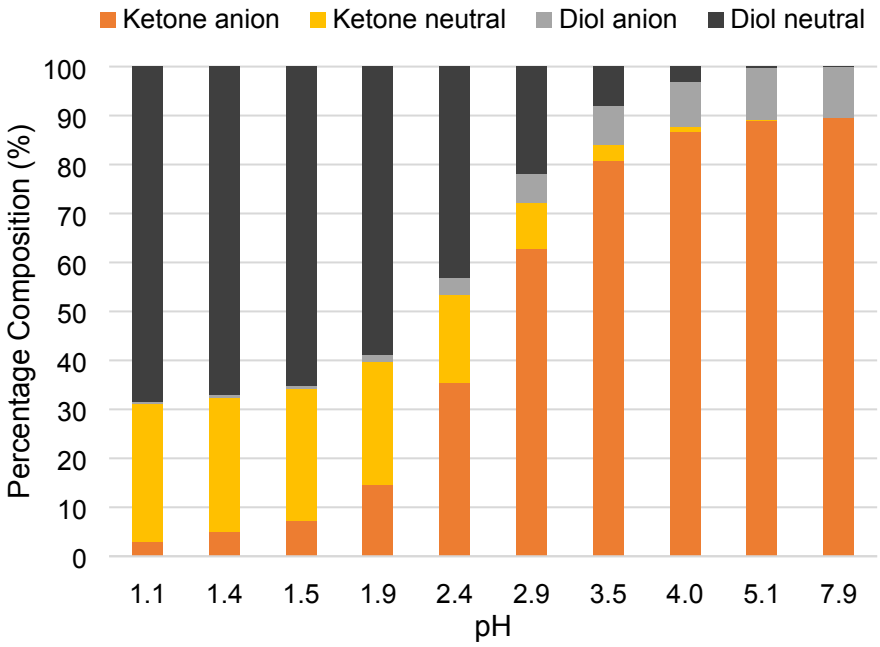

Figure 7: The relative percentage contributions of the anion and neutral forms of both ketone and diol forms of pyruvic acid at different pHs. The ketone versus diol form ratio was obtained from solution phase NMR. The anion versus neutral form ratio was obtained from calculations using the pK_a value of ketone and diol forms[55].

At very low pHs (below pH 2), the dominant form of pyruvic acid is the neutral diol form. The second major structure is the neutral ketone form. As the pH increases, the concentration of the neutral diol form decreases, and the anionic ketone form become more dominant. At pH 2.4 there are three major species: About 36 % of pyruvic acid is in the anionic ketone form, 17 % is in the neutral ketone form and 44 % is in the neutral diol form. The remaining 3 % is in the anionic diol form. The concentration of the anion diol form as a function of pH remains small, with the maximum concentration of 10 % at pH 7.9. At pH higher than 3 the main form is the anionic ketone form. Our results are in qualitative good agreement with the previously published data[23].

As discussed above, the main peak of the UV spectrum does shift only by a few nm if the pH of the solution is changed. As a starting point, we consider theoretically all four structures for the contribution to the experimental spectrum.

Absorbance of the diol forms:

Tables 3 and 4 show the vertical excitation energies for the anionic and the neutral diol form. The first excitation energy of neutral and the anionic diol form are 218 nm and 213 nm respectively. Those energies are far away from the experimental measured UV spectrum (and the atmospherically relevant region). The maximal move of the peak location upon hydration of the diol forms (see Supporting Information) is to 200 nm, still far away from the experimentally measured UV spectrum. Further solvation of the diol form might shift the peak, but most probably not by 100 nm to the red. Our calculation agrees well with literature values of the excitation energies of the monohydrated diol form[35] which predicts a red shift of 5 nm from the diol to the hydrated diol form. Therefore, both forms will not be considered further to contributing to the experimental spectra.

Table 3: Vertical excitation energies and properties for the neutral diol form of pyruvic acid using ADC(2)/cc-pVDZ.

State	Energy (eV)	Energy [nm]	Orbital Excitation	Description	Oscillator strength	Dipole moment (Debye)
S1	5.68	218	HOMO → LUMO 59 %	nπ*	0.00161527	0.82395276
S2	7.96	156	HOMO-1 → LUMO 67 %	ππ*	0.01497746	4.38263578

Table 4: Vertical excitation energies and properties for the anion diol form of pyruvic acid using ADC(2)/cc-pVDZ.

State	Energy (eV)	Energy (nm)	Orbital Excitation	Description	Oscillator strength	Dipole moment (Debye)
S1	5.83	213	HOMO → LUMO + 2 31 % HOMO → LUMO + 4 31 % HOMO - 2 → LUMO + 4 16 % HOMO - 2 → LUMO + 2 15 %	nπ*	0.00081994	5.378

S2	6.25	198	HOMO - 2 → LUMO + 2 33 % HOMO - 2 → LUMO + 4 31 % HOMO → LUMO + 2 16 % HOMO → LUMO + 4 14 %	nπ*	0.000 45123	7.236

Absorbance of the anionic and neutral ketone form:

As discussed above for the gas phase results, the ketone form of pyruvic acid absorbs around 360 nm and might therefore be responsible for the peak in the solution as well. From the NMR results for pH below 4 it is evident, that we need to consider both the ketone and the anionic form as contributing forms to the experimental spectrum. The vertical excitation energies and properties of the anionic form are tabulated in Table 5.

Table 5: Vertical excitation energies and properties for the anionic ketone form (gas phase) calculated using ADC(2)/cc-pVDZ.

State	Energy (eV)	Energy [nm]	Orbital Excitation	Description	Oscillator strength	Dipole moment (Debye)
S1	3.18	390	HOMO → LUMO 88%	nπ*	0.00000638	12.58
S2	3.80	327	HOMO-2 → LUMO 91%	nπ*	0.00000407	9.22

The first excited state of the anionic ketone is around 390 nm. The second excited state is around 330 nm, which is where the main peak is located at the UV spectrum of pyruvic acid in water solution. Although the energy fits very well to the experimental peak, the structure is the anionic form in the gas phase. Solvation of the anion in a polar medium such as water will stabilize the ground state and therefore the excitation energy of the solvated anion will certainly differ from the bare anion. Noteworthy is also, that the excitation energies in these tables are at 0 K, temperature effects will broaden the spectrum. The width of the spectrum can be obtained by running MD simulation at room temperature. The main movement seen along the molecular dynamics simulation is the change in the C-C-C-O dihedral angle. The C-C-C-O at the optimized structure are located in the same plane (flat configuration) and during the MD simulation they are distorted

and move out of plane. The width of the first excited state transition of the anion obtained from molecular dynamics simulation is depicted in Figure 8. The maximum of the peak is located at around 390 nm, which is the same as obtained by calculating the vertical excitation energy, see Table 5. The peak width measured at half height is around 30 nm. Therefore, the rotation along the dihedral angle at finite temperature broadens the peak.

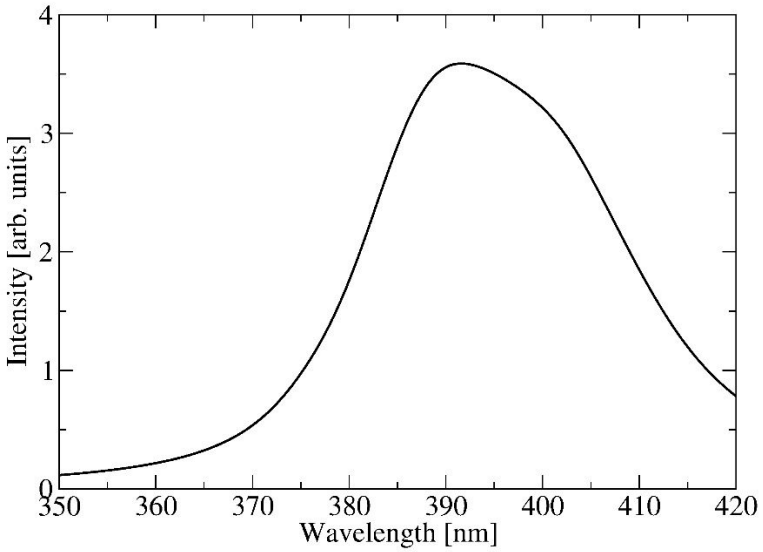

Figure 8: UV-Vis spectrum of first excited state transition for the anionic ketone obtained from gas phase molecular dynamics simulations obtained at the ADC(2)/cc-pVDZ level of theory using a Lorentzian line shape with of width of 0.05 nm.

In the following, we present excitation energies for anion ketone form pyruvic acid with different sized water clusters and we discuss the effect of hydration on the spectrum. The structures are shown in Figures 3 and 4. Structural properties of the structures were already discussed in the Methodology section (*vide supra*).

The excitation energies of the first excited state of each structure are summarized in Table 6.

Table 6: Vertical excitation energies and optical properties calculated by ADC(2)/cc-pVDZ method for the first excited state for the anion ketone embedded in clusters with up to 5 water molecules.

Number of water molecules	Energy (eV)	Energy [nm]	Description	Oscillator strength	Dipole moment (Debye)
0	3.18	390	nπ*	0.00000638	12.58
1	3.33	372	nπ*	0.00000065	9.96
2	3.34	371	nπ*	0.00000009	10.39
3	3.55	349	nπ*	0.00050326	12.09
4	3.74	331	nπ*	0.00040670	11.20
5	3.61	344	nπ*	0.00024242	27.08

From Table 6 it can be seen, that adding water molecules does shift the nπ* peak to the blue, from approximately 390 nm to 331 nm with 4 water molecules. Addition of the fifth water molecule shift to the red (344 nm). Interestingly to note, that the peak also gains in intensity. The effect of the first water molecule is a shift by 18 nm, whereas the second water molecule does not show this effect and the excitation energy is almost the same as for one water molecule. The third water molecule has a much larger effect and around 4 water molecules the excitation energy is 331 nm, already near to experimental peak at 320 nm. The natural transition orbitals involved in the excitation of the different clusters are very similar and are only located on the anion ketone pyruvic acid, and not on the water molecules. Molecular orbitals for both transitions are depicted in the Supporting Information. This is exemplified in Figure 9 for the anion and the anion with 4 water molecules.

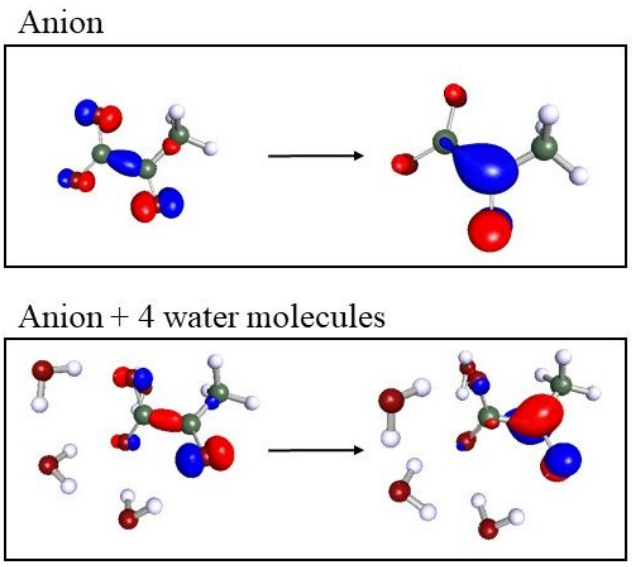

Figure 9: Natural transition orbitals involved in the first excitation transition of the anion and the anion cluster with 4 water molecules.

A closer inspection of the optimized structures shows that starting at the structure of the cluster involving 3 water molecules, the anion ketone pyruvic acid itself is not flat anymore. As discussed above, the change in the dihedral angle itself, does introduce broadening into the spectrum. Structures chosen for the vertical excitation energies are only one representative for a certain number of water molecules and thus hydrate size. Adding more and more water molecules to the solvated molecule, enlarges the number of possible contributing conformers. Therefore, considering only one structure for each hydrate size is not enough for quantitatively describing the shift, but gives a qualitative indication of the trend in the vertical excitation energy as a function of the number of water molecules. Therefore, performing molecular dynamics simulation does sample more conformers, and structures, and will lead to a more accurate description of the UV-Vis spectrum. Figure 10 shows the UV-Vis spectrum obtained from running molecular dynamics simulation on the anion with 4 water molecules.

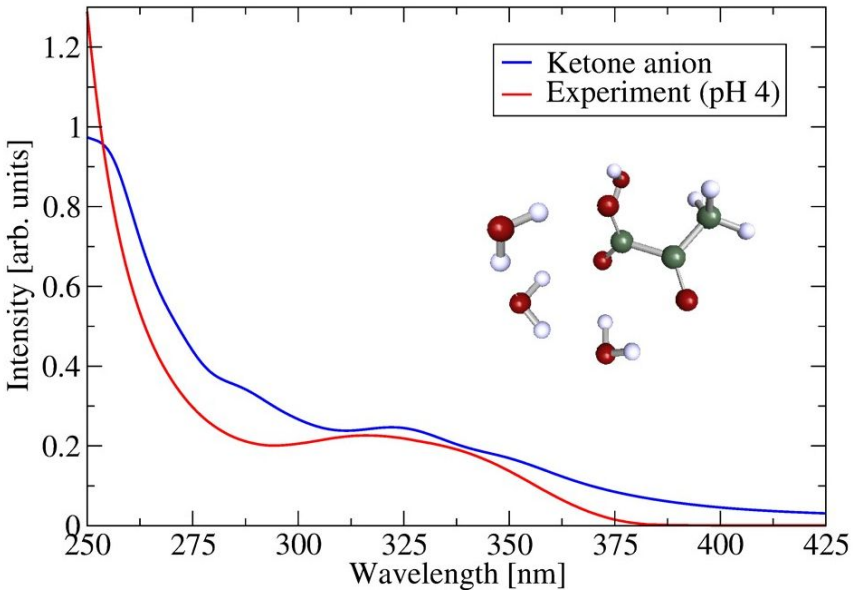

Figure 10: Comparison of UV-Vis spectrum obtained by running molecular dynamics simulation on the cluster of the anion with 4 water molecules (Lorentzian line shape width of 0.15 nm) with the experimental UV-Vis spectrum at pH 4.

The experimental spectrum is well described by the theoretical spectrum. The maximum of the peak at around 325 nm is predicted nicely by theory. The cluster size of anion and 4 water molecules can therefore serve as a good model system for the anion in water solution.

However, there is still a small discrepancy between the experimental and theoretical spectrum. For wavelengths greater than 375 nm, the experimental spectrum does not show any absorption, whereas the theoretical spectrum still shows a tail with non-zero absorption. This most likely is an artifact due to the limitation of the model we use. In order to correctly describe this region of the spectrum, larger water clusters, that resemble more pyruvic acid in water solution, most likely is necessary. On the other hand, for wavelength shorter than 260 nm, the experimental spectrum rises much more than the theoretical spectrum. This might be due to the following reasons: The theoretical spectrum takes into account only the first two excited states, higher lying states might be responsible for absorption in this spectral region. The other possibility might be that there are more species, such as for example protonation of the neutral pyruvic acid, the enol form of pyruvic acid or the diol forms, which might absorb as well but that are not included in our approach.

Additionally, the NMR analysis (see Figure 7) of the different species in the solution, gives a significant amount of neutral ketone form for pH values below 4. Therefore, we also address here the hydration effect of the neutral ketone form and its contribution to the spectrum. Figure 4 shows selected structures examined for the vertical excitation energy calculations.

Table 7 shows the vertical excitation energies associated with the structures depicted in Figure 4.

Table 7: Vertical excitation energies and optical properties calculated by ADC(2)/cc-pVDZ method for the first excited state for the neutral ketone embedded in clusters with up to 4 water molecules.

Number of water molecules	Energy (eV)	Energy (nm)	Description	Oscillator strength	Dipole moment (Debye)
0	3.47	358	nπ*	0.00000035	1.86
1	3.40	364	nπ*	0.00000439	3.20
2	3.46	359	nπ*	0.00000402	6.46
3	3.46	359	nπ*	0.00006370	3.00
4	3.58	347	nπ*	0.00021938	4.98

The effect of water on the excitation energy of the neutral ketone is less dominant than for the anion ketone. One water molecule does not significantly change the excitation energy. Work by Yang et, al[35] on the excitation energy of the ketone and ketone-water form predicts a blue shift of about 10 nm due to the hydration. The vertical excitation energies were calculated with a different method (TDDFT/6-31G+(d,p)) and are 373 nm for the ketone form, and 364 nm for the ketone-water complex. Their ketone-water structure is similar to the structure we have used, and to the structure predicted by Schnitzler et al. [37]. Our calculations predict a red shift of about 13 nm. Additional water molecules do not change much the excitation energy. Kakkar et al. have reported the two lowest conformers for the pyruvic acid with two water molecules cluster[34]. We have calculated the vertical excitation energies for both structures. Depicted is the Tc conformer, which is slightly higher in energy than the Tt conformer (by 0.22 ev). However, the excitation energy of both structures differs only by 3 nm, see supporting information. Also, here it is interestingly to

note, that addition of water does increase the oscillator strengths for the transition by about two orders of magnitude.

Our calculations predict only the excitation energy for one possible conformer. Adding additional water molecules increases the number of configurations possible, and this effect is not taken into account when calculating only the vertical excitation energy of one structure. The small differences in excitation energies shown in Table 7 might also arise from different C-C-C-O angle of pyruvic acid itself, as exemplified for the gas phase molecule.

In order to better understand the contribution of the ketone-water cluster to excitation spectrum, molecular dynamics simulation was performed. The spectrum is shown in Figure 11.

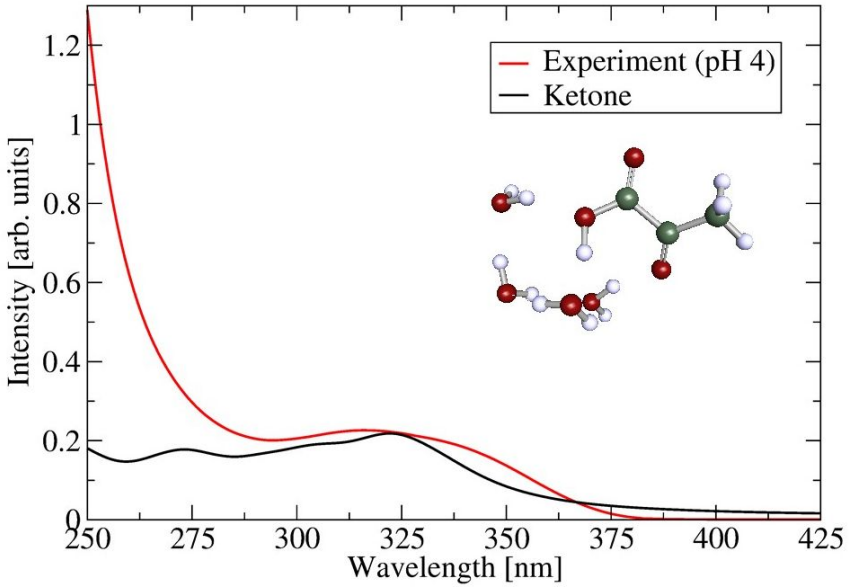

Figure 11: Comparison of UV-Vis spectrum obtained by running molecular dynamics simulation on the cluster of the ketone with 4 water molecules (Lorentzian line shape width of 0.15 nm) with the experimental UV-Vis spectrum at pH 4.

From Figure 11 it can be seen, that the ketone water complex does absorb at the 325 nm and therefore does contribute to the absorption of the experimental peak. The area around the peak is very well described by the theoretical spectrum. However, the prediction of the theoretical spectrum alone of the ketone with four water molecules misses the rise of the second excited state at lower wavelengths. In addition, for longer wavelength than 375 nm, there is a discrepancy

between the experimental and the theoretical spectrum. This might be due to the small size of the clusters we have employed, as discussed already above.

An improvement of the fit of the theoretical spectrum to the experimental spectrum can be achieved by a combination between the UV-Vis spectrum of the anion ketone with four water and the neutral ketone with four water molecules. The best predicted fit for the experimental spectrum occurs at 37.5 % ketone water cluster and 62.5 % anion ketone water cluster. The dominant contribution comes therefore from the anion ketone as also seen in the experimental obtained ratio at pHs around 4. However, the experimental obtained ratio predicts a much larger percentage of the anion ketone. The theoretical prediction uses a relatively small water cluster for describing the bulk solution, therefore an accurate ratio between the anion and the ketone water clusters cannot be expected. The theoretically predicted spectrum in Figure 12 describes very accurately the peak location at around 325 nm (compared to 316 nm from experimental results at pH 4) and the surrounded area. However, the rise of the second peak at lower wavelength is not well described. The theoretical spectrum uses two excitation states for calculating the spectrum. Inclusion of higher excited states might therefore be necessary for the correct description of the second excited state and for a better description of the area below 260 nm. Additionally, there might be more species such as protonated neutral pyruvic acid or the enol form of pyruvic acid, that should be included in the calculations in order to correctly describe the region below 260 nm. For wavelengths greater than 375 nm, the theoretical spectrum still shows a tail, whereas there is no absorption measured for the experimental spectrum. This might be due to usage of clusters of only 4 water molecules. A better description might be reached by employing much larger clusters that resemble more closely the local environment of pyruvic acid in solution.

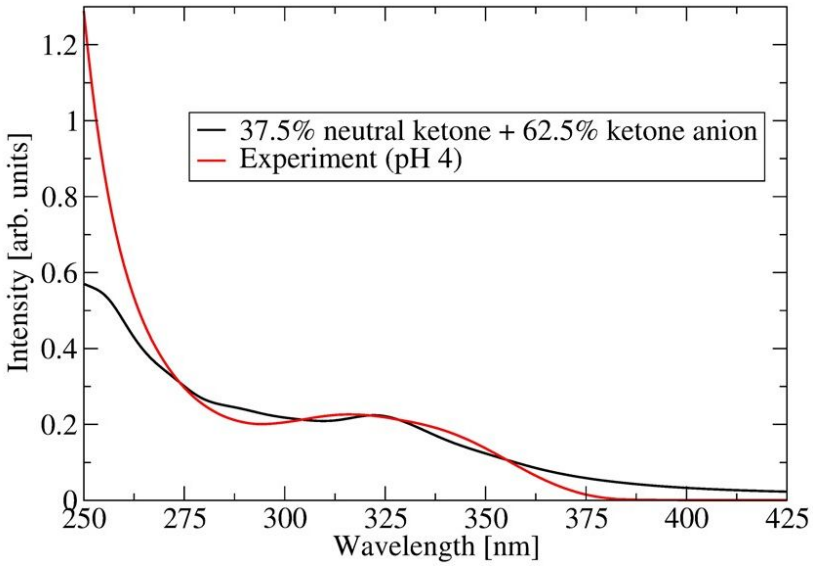

Figure 12: Combined theoretical spectrum obtained by running MD simulations on the ketone with four water molecules and the anion with 4 water molecules. The percentage is as follows: 37.5 % of the ketone water cluster spectrum combined with 62.5 % of the anion water cluster spectrum. The theoretical spectrum is compared to the experimental spectrum at pH=4.

Conclusions

Pyruvic acid exhibits conformational complexity in the gas phase and in water solvents. The gas phase UV spectrum can be explained by considering two conformers only. The Tc conformer, the global minimum, and the energetically nearby Tt conformer are both abundant in the gas phase, but the Tt conformer exists only at a small percentage. Both conformers absorb at around 360 nm, matching the experimentally observed peak. The transition is the first excited state and is of nπ* character. The second calculated excited state is at 235 nm and is also of nπ* character. However, the oscillator strength of this peak is much larger by at least two to three order of magnitudes. This is also seen in the experimental spectrum measured by several groups[21,61,62], as the UV absorbance rises towards 230 nm.

The UV spectrum in solution of pyruvic acid is characterized by a blue shift of 0.43 eV (40 nm difference in the peak location) of the main peak above 290 nm, the atmospherically relevant region. This peak cannot be explained by the gas phase results and therefore hydration of pyruvic acid needs to be considered explicitly. Solvation of pyruvic acids yields four different speciated

forms: neutral ketone and anion ketone form (loss of H^+) and their diol forms. ^1H NMR experiments have resolved the ratio of these conformers as a function of pH. At very low pHs the main species is the neutral diol together with neutral ketone (about 60 % of neutral diol and 30 % of neutral ketone). As the pH is increased, the anion ketone gains in percentage, and the neutral diol and neutral ketone distribution decreases. The anion diol, the fourth species, has a very low percentage at all pH values. This is consistent with previous speciation studies of Vaida and co-workers.[23] Another interesting conclusion from the aforementioned study is, that the photochemistry of solvated pyruvic acid depends on the pH of the solution. Thus, the initial solution composition defines the accessibility of different photochemical pathways.

Further, this study shows, that both diols forms have no absorbance at in the region from 280 nm to 400 nm and therefore in the calculations of the absorbance only the anion ketone form of pyruvic acid and the neutral ketone forms where considered. The peak is more shifted by hydration of the anion, since the water molecules do stabilize the negatively charged anion. The hydration effect on the ketone is less strong, but also here hydration does move the peak location. The structure of pyruvic acid itself (and its anion) in the hydrate also effects the peak location. It has been shown for the anionic ketone that non-flat structure of the backbone of pyruvic acid can change the peak by up to 30 nm. For larger number of water molecules used for hydration there exist more conformational minima, which are difficult to explore. Molecular Dynamics simulations are able to take into account different energetically accessible conformers for a certain temperature, and therefore are able to calculate their contributions to the UV spectrum. Vertical excitation energies for clusters up to five water molecules show already the correct trend of shifting the peak towards the blue. Molecular dynamics simulations of the anionic and neutral ketone form with four water molecules succeeds to correctly describe the experimental peak at 320 nm.

It is concluded from this study, that small hydrates with only four water molecules are able to reproduce the solvation effect of pyruvic acid. Two speciated forms were found to contribute to the excitation spectrum of pyruvic acid in water solution. The methodology employed here enables the characterization of the conformers, their speciated forms and their hydrates. Small cluster models are sufficient for describing the UV spectrum of solvated pyruvic acid correctly.

The effect of pH could not be modeled directly. The pH of a solution is the concentration of hydronium ions. The acid-base ratio is determined by the pH of the solution. This cannot be

described by the small size of the clusters employed. However, this can be modeled indirectly by assuming certain percentages of the acid form and its anionic form and combining their individual spectrum. For pyruvic acid this assumption lead to a very good description of the experimental UV spectrum.

The results encourage the study of other systems, such as aerosols, by small computational models. Speciated forms depending on the pH of the solution can be well described by our methodology. This gives insight into the molecular structures of solvated speciated forms, their dynamics over time and the location of the electronic excitation. Optical properties derived from different structures can be examined by investigation of the orbitals and the oscillator strengths of the transitions.

This study enables the investigation of atmospherically relevant molecules either in seawater or in the atmosphere with consideration of different conformers and of speciated forms. This study is a step towards investigating the experimental UV spectrum of solvated molecules, which depend on more than one species and/or conformers. The theoretical approach used here resolves the structures that contribute to the spectrum and gives insight into their optical properties. A combined theoretical and experimental approach is therefore proposed as a key tool in a better understanding and identification of more complex systems such as the constituents of aerosols. Identification of the constituents is important for follow up studies on their photodynamics and their impact on atmospheric chemistry and climate.

Acknowledgement:

The authors would like to gratefully acknowledge support by the National Science Foundation through the Center for Aerosol Impacts on Chemistry of the Environment funded under the Centers for Chemical Innovation Program Grant CHE1801971.

Supporting Information

The supporting information includes the effect of hydration on the vertical excitation energies to the first excited singlet state of the two diol forms (anionic and ketone), the depiction of the Tt conformer with two water molecules together with its optical properties, the comparison of the

vertical excitation energies and their optical properties for the neutral ketone and anionic form using different basis sets (i.e. def-SV(P) and cc-pVDZ) and the molecular orbitals for selected transitions., Additionally the cartesian coordinates for all structures discussed in this study has been provided.

References:

1 C. George, M. Ammann, B. D'Anna, D. J. Donaldson and S. A. Nizkorodov, *Chem. Rev.*, 2015, 115, 4218–4258.

2 C. George, B. D'Anna, H. Herrmann, C. Weller, V. Vaida, D. J. Donaldson, T. Bartels-Rausch and M. Ammann, Emerging areas in atmospheric photochemistry, *Top. Curr. Chem.*, 2014, **339**, 1–54.

3 V. Vaida, Spectroscopy of photoreactive systems: Implications for atmospheric chemistry, *J. Phys. Chem. A*, 2009, **113**, 5–18.

4 P. G. Eger, J. Schuladen, N. Sobanski, H. Fischer, E. Karu, J. Williams, M. Riva, Q. Zha, M. Ehn, L. L. J. Quéléver, S. Schallhart, J. Lelieveld and J. N. Crowley, Pyruvic acid in the boreal forest: first measurements and impact on radical chemistry, *Atmos. Chem. Phys. Discuss.*, 2019, 1–24.

5 K. Kawamura, E. Tachibana, K. Okuzawa, S. G. Aggarwal, Y. Kanaya and Z. F. Wang, High abundances of water-soluble dicarboxylic acids, ketocarboxylic acids and α-dicarbonyls in the mountaintop aerosols over the North China Plain during wheat burning season, *Atmos. Chem. Phys.*, 2013, **13**, 8285–8302.

6 M. O. Andreae, R. W. Talbot and S. M. Li, Atmospheric measurements of pyruvic and formic acid., *J. Geophys. Res.*, 1987, **92**, 6635–6641.

7 K. J. Zarzana, V. Selimovic, A. R. Koss, K. Sekimoto, M. M. Coggon, B. Yuan, W. P. Dubé, R. J. Yokelson, C. Warneke, J. A. De Gouw, J. M. Roberts and S. S. Brown, Primary emissions of glyoxal and methylglyoxal from laboratory measurements of open biomass burning, *Atmos. Chem. Phys.*, 2018, **18**, 15451–15470.

8 S. Tomaz, T. Cui, Y. Chen, K. G. Sexton, J. M. Roberts, C. Warneke, R. J. Yokelson, J. D. Surratt and B. J. Turpin, Photochemical Cloud Processing of Primary Wildfire Emissions as a Potential Source of Secondary Organic Aerosol, *Environ. Sci. Technol.*, 2018, **52**, 11027–11037.

9 E. A. Pillar and M. I. Guzman, Oxidation of Substituted Catechols at the Air-Water Interface: Production of Carboxylic Acids, Quinones, and Polyphenols, *Environ. Sci. Technol.*, 2017, **51**, 4951–4959.

10 J. M. Andino, J. N. Smith, R. C. Flagan, W. A. Goddard and J. H. Seinfeld, Mechanism of atmospheric photooxidation of aromatics: A theoretical study, *J. Phys. Chem.*, 1996, **100**, 10967–10980.

11 K. E. Altieri, A. G. Carlton, H. J. Lim, B. J. Turpin and S. P. Seitzinger, Evidence for

oligomer formation in clouds: Reactions of isoprene oxidation products, *Environ. Sci. Technol.*, 2006, **40**, 4957–4960.

12 B. Ervens, A. G. Carlton, B. J. Turpin, K. E. Altieri, S. M. Kreidenweis and G. Feingold, Secondary organic aerosol yields from cloud-processing of isoprene oxidation products, *Geophys. Res. Lett.*, , DOI:10.1029/2007GL031828.

13 A. G. Carlton, B. J. Turpin, H. J. Lim, K. E. Altieri and S. Seitzinger, Link between isoprene and secondary organic aerosol (SOA): Pyruvic acid oxidation yields low volatility organic acids in clouds, *Geophys. Res. Lett.*, , DOI:10.1029/2005GL025374.

14 A. E. Reed Harris, B. Ervens, R. K. Shoemaker, J. A. Kroll, R. J. Rapf, E. C. Griffith, A. Monod and V. Vaida, Photochemical kinetics of Pyruvic acid in aqueous solution, *J. Phys. Chem. A*, 2014, **118**, 8505–8516.

15 G. E. Hall, J. T. Muckerman, J. M. Preses, R. E. Weston and G. W. Flynn, Time-resolved FTIR studies of the photodissociation of pyruvic acid at 193 nm, *Chem. Phys. Lett.*, 1992, **193**, 77–83.

16 A. G. Rincón, M. I. Guzman, M. R. Hoffmann and A. J. Colussi, Optical absorptivity versus molecular composition of model organic aerosol matter, *J. Phys. Chem. A*, 2009, **113**, 10512–10520.

17 M. I. Guzmán, A. J. Colussi and M. R. Hoffmann, Photoinduced oligomerization of aqueous pyruvic acid, *J. Phys. Chem. A*, 2006, **110**, 3619–3626.

18 E. C. Griffith, B. K. Carpenter, R. K. Shoemaker and V. Vaida, Photochemistry of aqueous pyruvic acid, *Proc. Natl. Acad. Sci. U. S. A.*, 2013, **110**, 11714–11719.

19 J. A. O'Neill, T. G. Kreutz and G. W. Flynn, IR diode laser study of vibrational energy distribution in CO2 produced by UV excimer laser photofragmentation of pyruvic acid a, *J. Chem. Phys.*, 1987, **87**, 4598–4605.

20 D. Grosjean, Atmospheric reactions of pyruvic acid, *Atmos. Environ.*, 1983, **17**, 2379–2382.

21 S. Yamamoto and R. A. Back, The photolysis and thermal decomposition of pyruvic acid in the gas phase, *Can. J. Chem.*, 1985, **63**, 549–554.

22 R. S. Davidson, D. Goodwin and P. F. De Violet, The mechanism of the photo-induced decarboxylation of pyruvic acid in solution, *Chem. Phys. Lett.*, 1981, **78**, 471–474.

23 R. J. Rapf, M. R. Dooley, K. Kappes, R. J. Perkins and V. Vaida, PH Dependence of the Aqueous Photochemistry of α-Keto Acids, *J. Phys. Chem. A*, 2017, **121**, 8368–8379.

24 A. E. Reed Harris, A. Pajunoja, M. Cazaunau, A. Gratien, E. Pangui, A. Monod, E. C. Griffith, A. Virtanen, J. F. Doussin and V. Vaida, Multiphase Photochemistry of Pyruvic Acid under Atmospheric Conditions, *J. Phys. Chem. A*, 2017, **121**, 3327–3339.

25 A. J. Eugene and M. I. Guzman, Reactivity of Ketyl and Acetyl Radicals from Direct Solar Actinic Photolysis of Aqueous Pyruvic Acid, *J. Phys. Chem. A*, 2017, **121**, 2924–2935.

26 C. F. Wood, J. A. O'Neill and G. W. Flynn, Infrared diode laser probes of photofragmentation products: Bending excitation in CO2 produced by excimer laser photolysis of pyruvic acid, *Chem. Phys. Lett.*, 1984, **109**, 317–323.

27 S. Sutradhar, B. R. Samanta, R. Fernando and H. Reisler, Spectroscopy and Two-Photon Dissociation of Jet-Cooled Pyruvic Acid, *J. Phys. Chem. A*, 2019, **123**, 5906–5917.

28 Y. Fu, Y. Zhang, F. Zhang, J. Chen, Z. Zhu and X. Y. Yu, Does interfacial photochemistry play a role in the photolysis of pyruvic acid in water?, *Atmos. Environ.*, 2018, **191**, 36–45.

29 A. E. Reed Harris, J. F. Doussin, B. K. Carpenter and V. Vaida, Gas-Phase Photolysis of Pyruvic Acid: The Effect of Pressure on Reaction Rates and Products, *J. Phys. Chem. A*, 2016, **120**, 10123–10133.

30 X. P. Chang, Q. Fang and G. Cui, Mechanistic photodecarboxylation of pyruvic acid: Excited-state proton transfer and three-state intersection, *J. Chem. Phys.*, 2014, **141**, 154311.

31 G. Da Silva, Decomposition of Pyruvic Acid on the Ground-State Potential Energy Surface, *J. Phys. Chem. A*, 2016, **120**, 276–283.

32 J. Murto, T. Raaska, H. Kunttu and M. Räsänen, Conformers and vibrational spectra of pyruvic acid: an ab initio study, *J. Mol. Struct. THEOCHEM*, 1989, **200**, 93–101.

33 R. Kakkar, M. Pathak and N. P. Radhika, A DFT study of the structures of pyruvic acid isomers and their decarboxylation, *Org. Biomol. Chem.*, 2006, **4**, 886–895.

34 R. Kakkar, M. Pathak and P. Gahlot, Effect of aqueous solvation on the structures of pyruvic acid isomers and their reactions in solution: A computational study, *J. Phys. Org. Chem.*, 2008, **21**, 23–29.

35 D. Yang and L. Zhang, Excited-state hydrogen bonding dynamics of pyruvic acid and geminal-diol, 2,2-dihydroxypropanoic acid in aqueous solution: A DFT/TDDFT study, *J. Phys. Org. Chem.*, 2012, **25**, 1391–1394.

36 Y. Valadbeigi and H. Farrokhpour, Theoretical study on keto-enol tautomerism and isomerization in pyruvic acid, *Int. J. Quantum Chem.*, 2013, **113**, 2372–2378.

37 E. G. Schnitzler, N. A. Seifert, S. Ghosh, J. Thomas, Y. Xu and W. Jäger, Hydration of the simplest α-keto acid: A rotational spectroscopic and: Ab initio study of the pyruvic acid-water complex, *Phys. Chem. Chem. Phys.*, 2017, **19**, 4440–4446.

38 A. E. Reed Harris, M. Cazaunau, A. Gratien, E. Pangui, J. F. Doussin and V. Vaida, Atmospheric Simulation Chamber Studies of the Gas-Phase Photolysis of Pyruvic Acid, *J. Phys. Chem. A*, 2017, **121**, 8348–8358.

39 S. L. Blair, A. E. Reed Harris, B. N. Frandsen, H. G. Kjaergaard, E. Pangui, M. Cazaunau, J.-F. Doussin and V. Vaida, Conformer-Specific Photolysis of Pyruvic Acid and the Effect of Water, *J. Phys. Chem. A*, 2020, **124**, 1240–1252.

40 Y. Fang, D. Lesnicki, K. J. Wall, M. P. Gaigeot, M. Sulpizi, V. Vaida and V. H. Grassian, Heterogeneous Interactions between Gas-Phase Pyruvic Acid and Hydroxylated Silica

Surfaces: A Combined Experimental and Theoretical Study, *J. Phys. Chem. A*, 2019, **123**, 983–991.

41 S. A. Epstein, D. Shemesh, V. T. Tran, S. A. Nizkorodov and R. B. Gerber, Absorption spectra and photolysis of methyl peroxide in liquid and frozen water, *J. Phys. Chem. A*, 2012, **116**, 6068–6077.

42 D. Shemesh, R. Salomon, S. H. S. H. Kim, G. S. G. S. Tyndall, S. A. S. A. Nizkorodov and R. B. B. Gerber, Adjacent keto and enol groups in photochemistry of a cyclic molecule: Products, mechanisms and dynamics, *Chem. Phys.*, 2018, **515**, 177–186.

43 D. Shemesh and R. B. B. Gerber, Molecular Dynamics of Photoinduced Reactions of Acrylic Acid: Products, Mechanisms, and Comparison with Experiment, *J. Phys. Chem. Lett.*, 2018, **9**, 527–533.

44 K. L. Plath, K. Takahashi, R. T. Skodje and V. Vaida, Fundamental and overtone vibrational spectra of gas-phase pyruvic acid, *J. Phys. Chem. A*, 2009, **113**, 7294–7303.

45 C. Chen and S. F. Shyu, Theoretical study of glyoxylic and pyruvic acids: Rotamers and intramolecular hydrogen bonding, *J. Mol. Struct. THEOCHEM*, 2000, **503**, 201–211.

46 I. D. Reva, S. G. Stepanian, L. Adamowicz and R. Fausto, Combined FTIR Matrix Isolation and Ab Initio Studies of Pyruvic Acid: Proof for Existence of the Second Conformer, *J. Phys. Chem. A*, 2001, **105**, 4773–4780.

47 K. Saito, G. Sasaki, K. Okada and S. Tanaka, Unimolecular decomposition of pyruvic acid: An experimental and theoretical study, *J. Phys. Chem.*, 1994, **98**, 3756–3761.

48 E. D. Raczyńska, K. Duczmal and M. Darowska, Experimental (FT-IR) and theoretical (DFT-IR) studies of keto-enol tautomerism in pyruvic acid, *Vib. Spectrosc.*, 2005, **39**, 37–45.

49 G. B. Ellison, A. F. Tuck and V. Vaida, Atmospheric processing of organic aerosols, *J. Geophys. Res. Atmos.*, 1999, **104**, 11633–11641.

50 P. Tarakeshwar and S. Manogaran, An ab initio study of pyruvic acid, *J. Mol. Struct. THEOCHEM*, 1998, **430**, 51–56.

51 I. Reva, C. M. Nunes, M. Biczysko and R. Fausto, Conformational switching in pyruvic acid isolated in Ar and N2 matrixes: Spectroscopic analysis, anharmonic simulation, and tunneling, *J. Phys. Chem. A*, 2015, **119**, 2614–2627.

52 W. J. Ray, J. E. Katon and D. B. Phillips, Structure, hydrogen bonding and vibrational spectra of pyruvic acid, *J. Mol. Struct.*, 1981, **74**, 75–84.

53 J. R. Keeffe, A. J. Kresge and N. P. Schepp, Generation of simple enols by photooxidation. Keto-enol equilibrium constants of some aliphatic systems in aqueous solution, *J. Am. Chem. Soc.*, 2002, **110**, 1993–1995.

54 M. K. Maroń, K. Takahashi, R. K. Shoemaker and V. Vaida, Hydration of pyruvic acid to its geminal-diol, 2,2-dihydroxypropanoic acid, in a water-restricted environment, *Chem. Phys. Lett.*, 2011, **513**, 184–190.

55 M. Luo, D. Shemesh, M. N. Sullivan, M. R. Alves, M. Song, R. B. Gerber and V. H. Grassian, The Impact of pH and NaCl and CaCl2 Salts on the Speciation and Photochemistry of Pyruvic Acid in the Aqueous Phase, *J. Phys. Chem. A*, 2020, submitted.

56 T. J. Zuehlsdorff and C. M. Isborn, *Int. J. Quantum Chem.*, 2019, 119, e25719.

57 J. Tomasi, B. Mennucci and R. Cammi, Quantum Mechanical Continuum Solvation Models, *Chem. Rev.*, 2005, **105**, 2999–3094.

58 A. Warshel and M. Levitt, Theoretical studies of enzymic reactions: Dielectric, electrostatic and steric stabilization of the carbonium ion in the reaction of lysozyme, *J. Mol. Biol.*, 1976, **103**, 227–249.

59 E. Brunk and U. Rothlisberger, Mixed Quantum Mechanical/Molecular Mechanical Molecular Dynamics Simulations of Biological Systems in Ground and Electronically Excited States, *Chem. Rev.*, 2015, **115**, 6217–6263.

60 K. Hirano, H. Nakano, Y. Nakao, H. Sato and S. Sakaki, Photo absorption of p-coumaric acid in aqueous solution: RISM-SCF-SEDD theory approach, *J. Comput. Chem.*, 2017, **38**, 1567–1573.

61 A. Horowitz, R. Meller and G. K. Moortgat, The UV-VIS absorption cross sections of the α-dicarbonyl compounds: Pyruvic acid, biacetyl and glyoxal, *J. Photochem. Photobiol. A Chem.*, 2001, **146**, 19–27.

62 A. Mellouki and Y. Mu, On the atmospheric degradation of pyruvic acid in the gas phase, *J. Photochem. Photobiol. A Chem.*, 2003, **157**, 295–300.

63 C. E. Lund Myhre and C. J. Nielsen, Optical properties in the UV and visible spectral region of organic acids relevant to tropospheric aerosols, *Atmos. Chem. Phys. Discuss.*, 2004, **4**, 3013–3043.

64 N. V. Karimova, M. Luo, V. H. Grassian and R. B. Gerber, Absorption Spectra of Benzoic Acid in Water at Different pH and in the Presence of Salts: Insights from the Integration of Experimental Data and Theoretical Cluster Models, *Phys. Chem. Chem. Phys.*, 2020, **22**, 5046–5056.

65 X. Xu, J. Zheng and D. G. Truhlar, Ultraviolet Absorption Spectrum of Malonaldehyde in Water Is Dominated by Solvent-Stabilized Conformations, *J. Am. Chem. Soc.*, 2015, **137**, 8026–8029.

66 M. Barbatti, A. J. A. Aquino and H. Lischka, The UV absorption of nucleobases: semi-classical ab initio spectra simulations, *Phys. Chem. Chem. Phys.*, 2010, **12**, 4959–4967.

67 D. E. Romonosky, L. Q. Nguyen, D. Shemesh, T. B. Nguyen, S. A. Epstein, D. B. C. Martin, C. D. Vanderwal, R. B. Gerber and S. A. Nizkorodov, Absorption spectra and aqueous photochemistry of β-hydroxyalkyl nitrates of atmospheric interest, *Mol. Phys.*, 2015, **113**, 2179–2190.

68 M. J. Ezell, W. Wang, D. Shemesh, A. Ni, R. B. Gerber and B. J. Finlayson-Pitts, Experimental and Theoretical Studies of the Environmental Sensitivity of the Absorption Spectra and Photochemistry of Nitenpyram and Analogs, *ACS Earth Sp. Chem.*, 2019, **3**,

2063–2075.

69 A. V. Luzanov, A. A. Sukhorukov and V. E. Umanskii, Application of transition density matrix for analysis of excited states, *Theor. Exp. Chem.*, 1976, **10**, 354–361.

70 R. L. Martin, Natural transition orbitals, *J. Chem. Phys.*, 2003, **118**, 4775.

71 A. Lopalco, J. Douglas, N. Denora and V. J. Stella, Determination of pKa and Hydration Constants for a Series of α-Keto-Carboxylic Acids Using Nuclear Magnetic Resonance Spectrometry, *J. Pharm. Sci.*, 2016, **105**, 664–672.

72 K. M. Marstokk and H. Møllendal, Microwave spectrum, conformation, barrier to internal rotation and dipole moment of pyruvic acid, *J. Mol. Struct.*, 1974, **20**, 257–267.

73 C. E. Dyllick-Brenzinger, A. Bauder and H. H. Günthard, The substitution structure, barrier to internal rotation, and low frequency vibrations of pyruvic acid, *Chem. Phys.*, 1977, **23**, 195–206.

74 R. Meyer and A. Bauder, Torsional coupling in pyruvic acid, *J. Mol. Spectrosc.*, 1982, **94**, 136–149.

75 H. Hollenstein, F. Akermann and H. H. Günthard, Vibrational analysis of pyruvic acid and D-, 13C- and 18O-labelled species: Matrix spectra, assignments, valence force field and normal coordinate analysis, *Spectrochim. Acta Part A Mol. Spectrosc.*, 1978, **34**, 1041–1063.

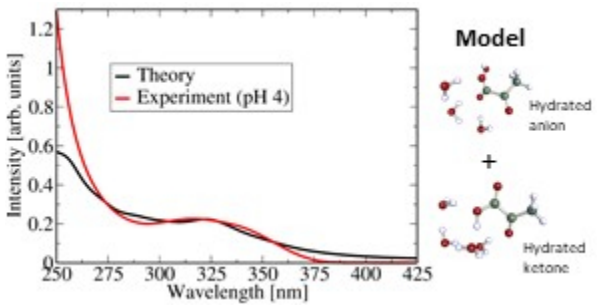

79x39mm (96 x 96 DPI)